Paper IV

THE JOURNAL OF GENE MEDICINE
J Gene Med 2006; **8**: 1131–1140.
Published online 29 June 2006 in Wiley InterScience (www.interscience.wiley.com) **DOI:** 10.1002/jgm.939

RESEARCH ARTICLE

Adeno-associated virus (AAV) serotypes 2, 4 and 5 display similar transduction profiles and penetrate solid tumor tissue in models of human glioma

Frits Thorsen[1,2,5]* †
Sandra Afione[3†]
Peter C. Huszthy[4]
Berit B. Tysnes[1,5]
Agnete Svendsen[4]
Rolf Bjerkvig[1,4,5]
Robert M. Kotin[3]
Per Eystein Lønning[4]
Frank Hoover[4]

[1]*Department of Biomedicine, Section of Anatomy and Cell Biology, University of Bergen, Bergen, Norway*

[2]*Department of Oncology and Medical Physics, Haukeland University Hospital, Bergen, Norway*

[3]*Laboratory of Biochemical Genetics, National Institutes of Health, Bethesda, MD, USA*

[4]*Section of Oncology, Department of Internal Medicine and the Hospital Program for Gene Therapy, Haukeland University Hospital, University of Bergen, Norway*

[5]*NorLux Neuro-Oncology, Department of Biomedicine, University of Bergen, Norway and Centre de Recherch Public Santé, Luxembourg*

*Correspondence to: Frits Thorsen, Department of Biomedicine, Jonas Lies vei 91, N-5009 Bergen, Norway. E-mail: frits.thorsen@biomed.uib.no

†These authors have contributed equally to this paper.

Received: 22 December 2005
Accepted: 30 March 2006

Abstract

Background Adeno-associated viral (AAV) vectors are potent delivery vehicles for gene transfer strategies directed at the central nervous system (CNS), muscle and liver. However, comparatively few studies have described AAV-mediated gene transfer to tumor tissues. We have previously demonstrated that while AAV2 and Adenoviral (Ad) 5 vectors have similar broad host ranges in tumor-derived cell lines, AAV2 was able to penetrate human glioblastoma biopsy spheroids and xenografts more efficiently than Ad 5 vectors. These results suggested that AAV vectors could be suitable for therapeutic gene delivery to solid tumor tissue. In the present work, the transduction efficacy of AAV serotypes 4 and 5 were compared to AAV2, both *in vitro* and in intracranial GBM xenografts derived from patient biopsies implanted into nude rats.

Methods AAV vector serotypes 2, 4, and 5 containing either the green fluorescent protein (GFP) or the bacterial β-galactosidase (*lacZ*) reporter gene were added to five different human glioma cell lines, to multicellular spheroids generated from glioblastoma patient biopsies, and to spheroids xenografted intracranially in nude rats. Transduction efficiency was assessed by fluorescence imaging, histochemistry, immunohistochemistry and flow cytometry.

Results While all three AAV serotypes were able to transduce the glioma cell lines when added individually or when they were administered in concert, AAV2 transduced the glioma cells most effectively compared to AAV4 or AAV5. Upon infecting glioblastoma spheroids *in vitro*, all three AAV serotypes efficiently transduced cells located at the surface as well as within deeper layers of the spheroids. In addition, similarly to what was observed for AAV2 [16], both AAV4 and AAV5 were able to transduce human glioblastoma xenografts implanted intracranially.

Conclusions In addition to the widely used AAV2 serotype, AAV4 and AAV5 serotypes may also be used to transduce biologically diverse glioma cell lines. They also penetrate and transduce solid human tumor tissue derived from patient biopsies. Therefore, the data presented here provide a proof of principle for developing AAV4 and AAV5 as treatment vehicles for human malignant gliomas. Copyright © 2006 John Wiley & Sons, Ltd.

Keywords gene therapy; glioblastoma multiforme; viral transduction; tumor spheroids; AAV2; AAV4; AAV5

Introduction

Genetic defects affecting cell growth arrest and apoptosis play a critical role promoting carcinogenesis as well as growth of established cancers. Therefore, novel strategies including gene transfer to malignant cells have been explored as anti-cancer therapy [1]. However, while pre-clinical data have been promising, results from early clinical trials utilizing systemic or local application of viral vectors have proven to be disappointing. A key problem for cancer gene therapy is insufficient transduction due to ineffective systemic delivery and inadequate tissue penetration [2,3]. In addition, disseminated cancers present a particular challenge for systemic gene delivery as they require efficient tissue penetration in metastatic deposits. Thus, there is a need to identify and develop more effective delivery systems.

Adeno-associated virus (AAV) belongs to the parvovirus family and contains a single-stranded DNA genome of about 4.7 kb [4–6]. To date, AAVs have not been associated with any human disease and have shown superior safety profiles in pre-clinical animal studies as well as in human trials [7–11]. Moreover, AAV2 vectors have favorable properties for cancer gene therapy, including a broad host range [12–15] and the ability to penetrate solid tumor tissue [16,17]. Although recombinant AAV vectors are typically maintained episomally in host cells [18], it is well recognized that also some chromosomal integration does occur, thus maintaining the therapeutic gene in progeny cells [19].

A family of distinct AAV serotypes has been identified (AAV1 to 8) [20–24]. Although the genomic organization of each serotype is similar, the AAV serotypes differ in their coding sequences. These differences are considered to influence their biological behavior such as binding to cell-surface molecules. Previous studies have established that the various AAV serotypes have distinct host ranges in different tissues [25]. Accordingly, current evidence suggests that while AAV2 binds to heparan sulfate proteoglycans and co-receptors [26–29], AAV4 and AAV5 bind to distinct sialic acid containing glycoproteins, and AAV5 may utilize platelet-derived growth factor receptor PDGFR [30–32].

Gliomas are derived from glia (supportive) cells in the central nervous system (CNS). They show localized, infiltrative growth within the brain. The most malignant form, glioblastoma multiforme (GBM), displays extensive cellular heterogeneity, characterized by numerous atypical cells, extensive cell division, angiogenesis and necrosis. There is an urgent need for new treatment strategies, as the current prognosis remains poor [33].

The AAV2, AAV4 and AAV5 serotypes were chosen for evaluation since previous evidence suggests that they may be permissible to different cell populations in the CNS [34]. It has been shown that AAV2 preferentially transduces neurons, whereas AAV4 is most efficient in ependymal cells. AAV5 transduces both neurons and glial cells [34–36]. In addition, the identified AAV receptors have been shown to be expressed in glioma cell lines and GBM tissue [37]. Evaluation of the transduction ability of these AAV serotypes would reveal which AAV is the most efficient for gene delivery to GBM tissue. Moreover, this knowledge may have pertinent clinical relevance, since neutralizing antibodies against the first choice of AAV serotype may be present in certain individuals [24]. Since the blood-brain barrier is disrupted in high-grade gliomas and neurosurgical intervention further increases the access of peripheral blood to the tumor site, the presence of neutralizing antibodies is a factor to consider for brain tumor therapy as well. In the present study, the host ranges of AAV2, AAV4 and AAV5 in five different human glioma cell lines were assessed. Next, the abilities of the three AAV serotypes to transduce and penetrate solid tumor tissue derived from patient biopsies was examined using an *in vitro* spheroid model. Finally, these vectors were tested *in vivo* by transducing human GBMs xenografted intracranially in nude rats.

Materials and methods

Vector production

293 T cells (Adenovirus type (Ad) 5 transformed human embryonic kidney cells containing the SV40 large T antigen) were maintained in Dulbecco's modified Eagle's medium (DMEM) containing 25 mM glucose, 100 μg/ml streptomycin, 100 U/ml penicillin, and 10% fetal bovine serum (FBS). For vector production, 293 T cells were seeded at a density of 7×10^6 cells/15-cm plate the day before transfection. All transfections were performed by calcium phosphate co-precipitation.

Recombinant AAV2 vectors were generated by co-transfecting 15 μg of an AAV expression plasmid containing the nuclear-targeted β-galactosidase gene (AAVRnLacZ) [38], or the gene for the green fluorescent protein (GFP), with 45 μg of the adenoviral helper packaging plasmid pDG (generous gift from Prof. J. A. Kleinschmidt) [39].

For recombinant AAV4 vector production, the transfection was performed using 32 μg/plate of the Ad 5-derived helper plasmid pSR449B [40], 20 μg/plate of AAVRn-LacZ, or an expression vector containing the GFP gene and 20 μg/plate of pSV40oriAAV$_{4-2}$ containing AAV4 *rep* and *cap* sequences [21]. To generate AAV5 vectors, 32 μg/plate of pSR449B, 20 μg/plate of AAV5-nlacZ [20], also expressing the nuclear-targeted β-galactosidase gene or the nuclear-targeted green fluorescent protein (nGFP) gene, and 20 μg/plate of the Rep-Cap helper plasmid [41] was delivered to the cells.

The expression cassette was flanked by AAV2 inverted terminal repeat (ITR) sequences for the AAV2-nlacZ or AAV2-GFP particles and for the AAV4-nlacZ or AAV4-GFP particles. For AAV5-nlacZ or AAV5-nGFP particles, the expression cassette was flanked by AAV5 ITR sequences (Figure 1). Forty-eight hours after transfection, the cells

DOI: 10.1002/jgm

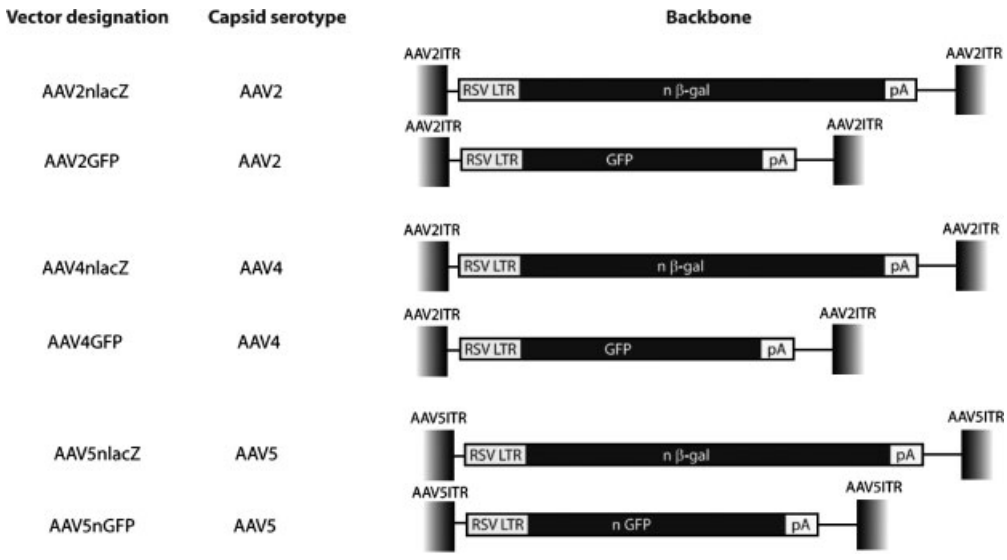

Figure 1. Schematic diagram of AAV vector constructs. Each vector contained a reporter gene, either the nuclear-targeted *β*-galactosidase (n*lacZ*) or the green fluorescent protein (GFP or nuclear-targeted GFP) gene. Reporter gene expression was driven by Rous sarcoma virus long terminal repeat (RSV LTR) sequences. AAV2 and AAV4 serotype vectors were made using inverted terminal repeat (ITR) sequences derived from AAV2, whereas AAV5 contained AAV5 ITR sequences. The vectors contained synthetic poly A sequences contained in the pAAVRnLacZ plasmid [29]

were harvested and lysed by three cycles of freezing and thawing followed by low-speed centrifugation to remove cellular debris. Sodium deoxycholate and 300 U/ml benzonase (Sigma, St. Louis, MO, USA) were added to the cell lysate and incubated for 1 h at 37 °C. DNase-resistant encapsidated AAV particles were purified by isopycnic banding in a CsCl density gradient. The purified gradient was extensively dialyzed against phosphate-buffered saline (PBS) containing 2 mM $MgCl_2$, and the particle concentration (titer) was determined by real-time quantitative polymerase chain reaction (PCR) using an ABI PRISM 7700 sequence detection system (Applied Biosystems, Foster City, CA, USA), the SYBR Green PCR Master Mix (Applied Biosystems) and a specific primer pair for the Rous sarcoma virus (RSV) promoter. Vector aliquots were stored at – 70 °C and routinely contained $1 \times 10^{9-11}$ genomes/ml.

Cell culture and preparation of spheroids

The human glioma cell lines A172, D37, GaMg, HF-66 and U373 as well as glioblastoma biopsy spheroids were grown in DMEM supplemented with 10% heat-inactivated FBS. The medium contained four times the prescribed concentration of non-essential amino acids, 2% L-glutamine, penicillin (100 IU/ml) and streptomycin (100 µg/mL, all biochemicals from BioWhittaker, Verviers, Belgium). Spheroids were prepared from glioblastoma multiforme patient biopsy material as described previously [42]. The cell lines and the spheroids were incubated in 80-cm^2 culture flasks (Nunc, Roskilde, Denmark), and grown in a water-jacketed incubator at 37 °C (100% relative humidity, 5% CO_2). All patients gave their oral informed consent regarding the use of human material in this project. The study was approved by the Regional Ethical Committee.

Viral transduction

For each glioma cell line, 1×10^5 cells were plated in 2 mL medium in each well of a 6-well plate (Nunc). The cells were allowed to attach for 24 h, and the number of cells/well was verified by enzymatic detachment followed by counting in a Bürcher chamber. Vector samples diluted in Dulbecco's phosphate-buffered saline (DPBS; BioWhittaker) with 1% D-glucose (Merck, Darmstadt, Germany) were added to cultures at a concentration of 500 vector genomes per cell. Three days post-infection, the cells were processed for flow cytometry, as described below. Glioblastoma spheroids (200–300 µm in diameter) from seven patients were kept individually in 200 µL medium in 96-well plates (Nunc). CsCl-gradient purified AAV particles containing 2×10^8 of AAV2-GFP genomes, 2×10^7 or 2×10^8 of AAV4-GFP genomes, or 2×10^7 or 1×10^9 of AAV5-GFP genomes were added to each well (4–6 spheroids for each serotype). Infection was allowed to proceed overnight, whereafter the growth medium was changed weekly.

Quantification of AAV serotype transduction efficiency in monolayer cultures

The percentage of viral transduction in monolayer cultures was determined by flow cytometric analysis as described previously [16]. Briefly, cells were detached

DOI: 10.1002/jgm

with 500 μL of 0.025% trypsin (BioWhittaker) and, after 5 min of incubation, protease activity was inhibited by adding 500 μL complete medium. The cell suspension was centrifuged at 140 *g* for 4 min at 4 °C. The supernatant was removed, and the cells were re-suspended in 1 mL DPBS with 1% D-glucose (Merck). The cell suspensions were kept on ice until flow cytometric analysis. The percentage of GFP-expressing cells was determined using a FACSort flow cytometer (Becton Dickinson, San Jose, CA, USA). The fluorescence intensities were quantified by gating a two-parameter forward- and side-scatter cytogram to a one-parameter green fluorescence intensity plot. Milli-Q water and DPBS were both used as negative controls. To reduce intra-assay deviation, three independent experiments were performed. In each experiment, each sample was assayed in triplicate. A total of 5000 gated cells were collected for each fluorescence intensity histogram. These intensity distributions showed that transduced cell populations were skewed towards higher mean intensities compared to the controls. The flow cytometry channel harboring the maximum fluorescence intensity value in each histogram was recorded. Thus, each histogram obtained from untransduced cells was subtracted from the histogram of the respective transduced cells, and the number of cells in the resulting population was defined as the percent of transduced cells. In the resulting histograms the number of transduced cells was calculated within a defined region to the right of the control histogram peak (around channel 10). For each intensity histogram, the flow cytometry channel harboring the maximum intensity value (FL1 value) was also recorded.

Confocal laser scanning microscopy (CLSM) of monolayer cultures and multicellular spheroids

The extent of GFP expression in the infected monolayer cultures and glioblastoma spheroids was determined by visual inspection using confocal laser scanning microscopy (TCS NT; Leica, Heidelberg, Germany) with an argon-krypton laser. The monolayers were examined 3 to 7 days post-infection with transmission light in combination with FITC and Hoffman filter optics. Confocal images were captured in areas of the monolayers expressing the highest fluorescence intensity.

The spheroids were transferred to a glass slide in one drop of DPBS with 1% D-glucose 14 days post-infection, and examined under the microscope. A total of 64 optical sections covering 166 μm (each section with a resolution of 512 × 512 pixels) from each spheroid were recorded using identical gain settings. The gain was deliberately set to exhibit a weak auto-fluorescence on the negative controls. The sections were superimposed into a single image to produce the final image. Uninfected spheroids were used as negative controls.

GBM xenograft models: generation and vector delivery

Xenograft models were prepared in rnu-/rnu- nude rat hosts (150 g weight, both male and female animals were used) as previously described [16]. Glioblastoma multiforme spheroids derived from three different patient biopsies were used in these experiments. Prior to surgery, the animals were anesthetized with a subcutaneous injection of fentanyl/fluanisone/midazolam at a dose of 0.15 mg/kg body weight and secured in a Kopf model 900 small animal stereotactic frame (David Kopf Instruments, Tujunga, CA, USA). In addition, local anaesthetic (1 ml of Xylocaine, 20 mg/mL solution) was given subcutaneously prior to operation. After incision of the skin with a sterile surgical blade, the skin flaps were withdrawn to reveal the sagittal and the coronal sutures. A burr hole was prepared with a dental drill at 3 mm to the right of the sagittal suture and 1 mm posterior to the bregma. Twenty regular-shaped spheroids of approximately 400 μm diameter were delivered by a Hamilton syringe to the cortex at a depth of 2.5 mm measured from the dura mater. After injection, the syringe was left in place for 10 min before retracting the needle to avoid backflow of the spheroids. The skin folds were closed with polyamide surgical thread. After surgery, the animals were allowed to recover in an incubator set at 35 °C before returning them to their cages, followed by daily observations.

In order to confirm presence of tumor in the rat brain before vector injections, the animals were examined with a Siemens MAGNETOM Vision Plus 1.5 Tesla clinical magnetic resonance (MR) scanner (Siemens, Erlangen, Germany) equipped with a 25 mT/m gradient system, and a standard small circular coil. T1- and T2-weighted images were taken as previously described [43].

Three weeks post-implantation, the animals were anaesthesized and prepared for vector injection. AAV2 (n = 7 xenografts), AAV4 (n = 4 xenografts) or AAV5 vectors (n = 4 xenografts) containing GFP or *lacZ* transgenes were injected. The skin was withdrawn to reveal the location of the craniotomy. Volumes of 10 μl of AAV vector preparation were drawn up in a 10-μL Hamilton glass syringe with a 26-gauge needle. The needle was secured in a microprocessor controlled infusion pump (UMP 2–1, World Precision Instruments, Stevenage, UK), connected to the stereotactic frame. The needle tip was navigated to the site of craniotomy and inserted at the same coordinates as used for spheroid implantation. Two injections with 10 μl vector stock were performed. The infusion flow rate was 20 μl/h. After infusion, the needle was left in place for 10 min in order to avoid reflux of the injected fluid. The needle was carefully and slowly retracted, and the skin folds were closed with polyamide surgical thread. Following surgery, rats were allowed to recover in an incubator set at 35 °C before being returned to their cages. The animals were sacrificed upon tumor-related neurological symptoms (2–3 months post-implantation). The handling of the animals and the

DOI: 10.1002/jgm

surgical procedures were performed in accordance with the Norwegian Animal Act.

Beta-galactosidase staining and HRP immunohistochemistry

Whole brains (resected from sacrificed animals) or spheroids were embedded in Tissue Tek media (Sakura Finetek Europe B.V., Zoeterwoude, The Netherlands) and rapidly frozen in liquid nitrogen. Axial cryosections 12–18 μm thick were cut using a Leica cryotome. Cryosections of monolayers or spheroids were fixed for 15 min in 0.2% glutaraldehyde and 2% formaldehyde in PBS containing 2 mM Mg^{2+} at 25 °C. Specimens were rinsed in PBS/Mg buffer thrice for 5 min each. The X-gal reaction buffer contained 1 mg/mL X-gal, 5 mM $K_4Fe(CN)_6$, 5 mM $K_3Fe(CN)_6$ and 2 mM $MgCl_2$ dissolved in PBS (pH 7.4) as described previously [16]. The solution was filtered through a 0.45-μm syringe filter before use (Pall Gelman Laboratory, Lane Cove, UK). Cells and sections were stained either for 4 h at room temperature or at 4 °C overnight. The sections were counterstained with haematoxylin and eosin, and examined using light microscopy. Fixed brain tumor sections from the xenografted animals were probed with an anti-GFP antibody (Chemicon AB3080 dilution 1 : 100; Chemicon International, Inc., Temecula, CA, USA) and incubated with horse radish peroxidase (HRP)-conjugated secondary antibodies (DAKO envision kit K4007; DakoCytomation, Glostrup, DK) before detection in a DAB reaction (DAKO envision kit) according to the manufacturer's instructions.

Results

Quantification of AAV serotype transduction efficiency in monolayer cultures

Differences in transduction efficiency were detected by flow cytometric analyses of the infected cell lines. The flow analyses confirmed the visual observations, showing each cell line to be transduced by each of the AAV serotypes. Typical fluorescence intensity histograms for one of the cell lines (U373) infected with the three AAV-GFP serotypes are displayed in Figure 2A. The data revealed that the AAV2 vectors yielded the overall best transduction rates varying between 15% and 66%, while both the AAV4 and the AAV5 vectors transduced the glioma cells in the range of 4–14% (Figure 2B). The results showing the mean FL1 channels confirmed the transduction data (Figure 2C).

Simultaneous transduction by AAV vectors

In order to evaluate if AAV2, 4 and 5 serotypes could transduce the same cells, GaMg glioma cells were simultaneously infected with two different AAV serotypes, each expressing a different reporter gene. Following infection, histochemistry was performed in order to identify *lacZ*-expressing cells. Thereafter, double-labelled cells (GFP and *lacZ*) were scored using both fluorescent and light microscopy. By using this combinatorial approach, we found that AAV2, 4 and 5 vectors were able to transduce the same cells (Figure 3).

Transduction of human glioblastoma spheroids by AAV serotypes

To evaluate if AAV4 and AAV5 could penetrate solid tumor tissue similarly to AAV2 [16], the vectors were added to glioblastoma spheroids. The spheroids were confirmed to be viable in long-term culture using a standard Live/Dead two-color staining assay (Molecular Probes, Eugene, OR, USA; data not shown). Following infection with AAV particles containing the GFP or the lacZ transgene, the spheroids were cultured for up to 3 months. GBM spheroids (diameter from 150–200 μm) derived from patient biopsy specimens were examined for green fluorescence by CLSM at various time intervals. *lacZ*-positive cells were assessed following cryosectioning and histochemical processing.

Interestingly, it was observed that all infected spheroids displayed positive reporter gene signals, irrespective of the genetic diversity displayed by the individual biopsies. AAV2-GFP exhibited the highest ability to transduce individual cells within the tumor spheroids (Figures 4A and 4B, data shown for two different specimens). Positive signals were also observed from the AAV4-GFP vector (Figures 4C and 4D). The least signal was observed from the AAV5 vector (Figure 4E). However, this result was partially dose-dependent since a 50-fold increase in vector genomes elevated the fraction of AAV5-GFP-positive cells (Figure 4F). When generating optical sections from the spheroid centers using CLSM, we observed positive signals from cells transfected with all serotypes (data shown for AAV4, Figure 4G). The auto-fluorescence of uninfected spheroids was low (Figure 4H). AAV vectors expressing the *lacZ* reporter gene (AAV2, AAV4 and AAV5) and the nGFP (AAV5) reporter gene also transduced spheroids, and validated the transduction profiles observed with the GFP reporter gene (data not shown).

AAV transduction of GBM xenografts *in vivo*

The transduction patterns of the different AAV serotype vectors were examined *in vivo* using a xenograft model prepared from human GBM tumor spheroids. As these xenografts were generated from patient biopsy material and not from immortalized cell lines, they retained the heterogeneity and characteristics of glioblastoma multiforme *in situ* [43].

The results of the stereotactic injections of AAV vectors into established xenografts in nude rat brains

DOI: 10.1002/jgm

A

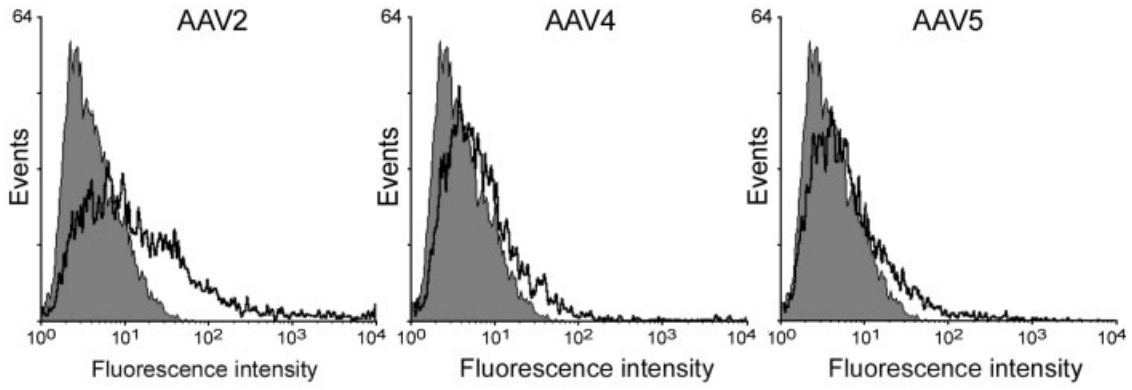

B

Cell Line	AAV2 % Transduction	AAV4 % Transduction	AAV5 % Transduction
A172	65.5 ± 5.2	6.1 ± 3.5	11.4 ± 10.6
D37	60.9 ± 2.0	4.8 ± 2.3	3.9 ± 1.6
GaMg	14.9 ± 1.3	6.0 ± 3.4	5.8 ± 3.4
HF-66	31.3 ± 8.7	11.8 ± 6.8	6.6 ± 3.7
U373	42.6 ± 5.3	14.1 ± 4.6	10.6 ± 2.2

C

Cell Line	Control Mean FL1 Channel	AAV2 Mean FL1 Channel	AAV4 Mean FL1 Channel	AAV5 Mean FL1 Channel
A172	4.7 ± 0.3	65.0 ± 6.4	5.8 ± 0.7	7.3 ± 0.8
D37	4.9 ± 0.3	83.1 ± 7.3	7.1 ± 0.7	5.7 ± 0.3
GaMg	8.0 ± 0.4	22.8 ± 2.3	8.3 ± 0.5	8.3 ± 0.6
HF-66	8.7 ± 1.0	60.4 ± 9.2	13.7 ± 1.9	11.5 ± 1.3
U373	5.8 ± 0.7	188.6 ± 23.7	26.0 ± 5.5	16.5 ± 3.0

Figure 2. AAV vectors transduce human glioma cell lines at different efficiencies. Five glioma cell lines were infected with the AAV serotypes 2, 4 and 5 at a concentration of 500 vector genomes per cell. Shown here are representative histograms for the U373 cell line. Similar histograms were obtained for all five human glioma cell lines. (A) Flow cytometry intensity histograms for transduced cells were compared with a negative control (untransduced cells). The transduced cell populations were skewed towards higher mean intensity values, compared to the negative control (grey, filled histograms). (B) The fluorescence intensity histograms of the untransduced cells were subtracted from the fluorescence intensity histograms of the transduced cells, and the percent transduction was calculated. The results from these calculations are shown (mean ± standard error of the mean (SEM)). (C) For each fluorescence intensity histogram obtained, the channel on the flow cytometer harboring the highest FL1 intensity value was recorded, and the mean FL1 channel was thereafter calculated (mean ± SEM)

are shown in Figure 5. The presence of intracranial tumors prior to vector injections was verified using T1-weighted MR acquisitions with contrast enhancement (Figure 5A). The histological evaluation showed that AAV2 was able to transduce the tumor cells around the injection site (Figure 5B). However, a widespread AAV transduction throughout the tumor area was not seen. Similar results were obtained with AAV4 (Figure 5C) and AAV5 (Figure 5D), showing transduction in small clusters within the central part of the tumors. Control sections of rat brains stained for the GFP gene product showed no positive cells (data not shown).

Discussion

Due to the inadequate penetration and transduction abilities of many vector systems in solid tumor tissue, the lack of effective delivery systems still remains a limitation for cancer gene therapy [3,16,45]. The observation that AAV2 vectors transduce and penetrate deep layers of biopsy tumor tissue provides a proof of principle for the application of these vectors for gene delivery to cancer tissues [1,17]. Here, we show that AAV serotypes 4 and 5, similarly to AAV2, display broad tropism for glioma cells. Despite the biological heterogeneity presented in the

DOI: 10.1002/jgm

models, our results show that the AAV2, 4 and 5 serotypes are each capable of transducing a range of human glioblastoma-derived cell lines as well as penetrating spheroids prepared from glioblastoma patient biopsies. Importantly, these characteristics were also observed when the AAV vectors were injected intracranially into GBM xenografts *in vivo*.

It has previously been shown that recombinant AAV serotypes 2, 4 and 5 transduce different cell types within the normal brain [34–36]. Based on these observations, we postulated that each AAV serotype would transduce different tumor phenotypes, thus providing a 'serotype signature'. However, our experiments showed that AAV2, AAV4 and AAV5 may transduce a large and overlapping spectrum of glioma cell lines and biopsies. One clear-cut explanation to account for the widespread transduction profile of the various AAV serotypes is that the different AAV receptors are widely expressed by glioma cells. This contention is supported by previous experiments showing that the attachment molecules for AAV2, AAV4 or AAV5 are expressed in human glioblastoma cells and biopsy specimens [37,46]. These observations may have important implications for future therapeutic interventions. Previous studies have indicated

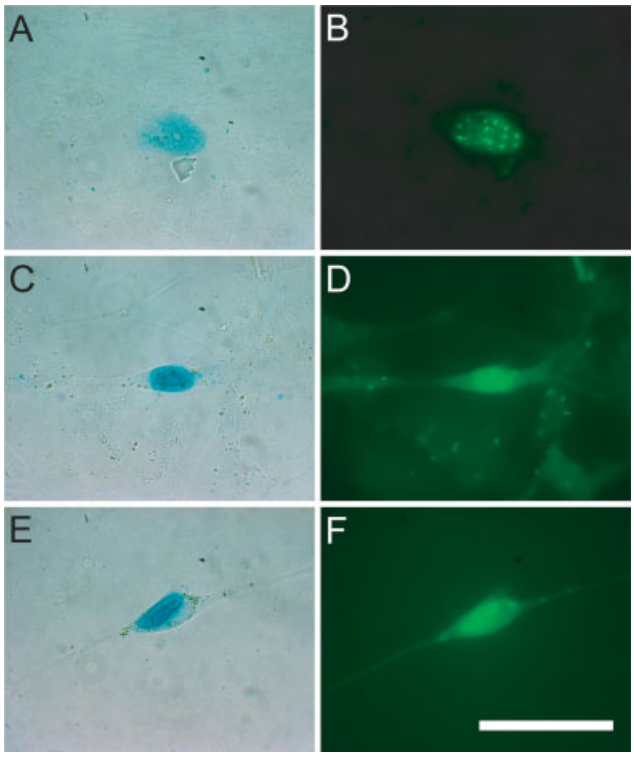

Figure 3. AAV 2, AAV4 and AAV5 are able to simultaneously transduce glioma cells. GaMg glioma cells were simultaneously transduced with two AAV serotype vectors encoding GFP and *LacZ* transgenes. Five days post-transduction, the cells were assessed for expression of both transgenes, using fluorescence and transmission microscopy. Simultaneous transduction with AAV2nLacZ (A) and AAV4-GFP (B); simultaneous transduction with AAV4nLacZ (C) and AAV5-nGFP (D); simultaneous transduction with AAV5nLacZ (E) and AAV2-GFP (F). Magnification: 800×; scale bar: 50 μm

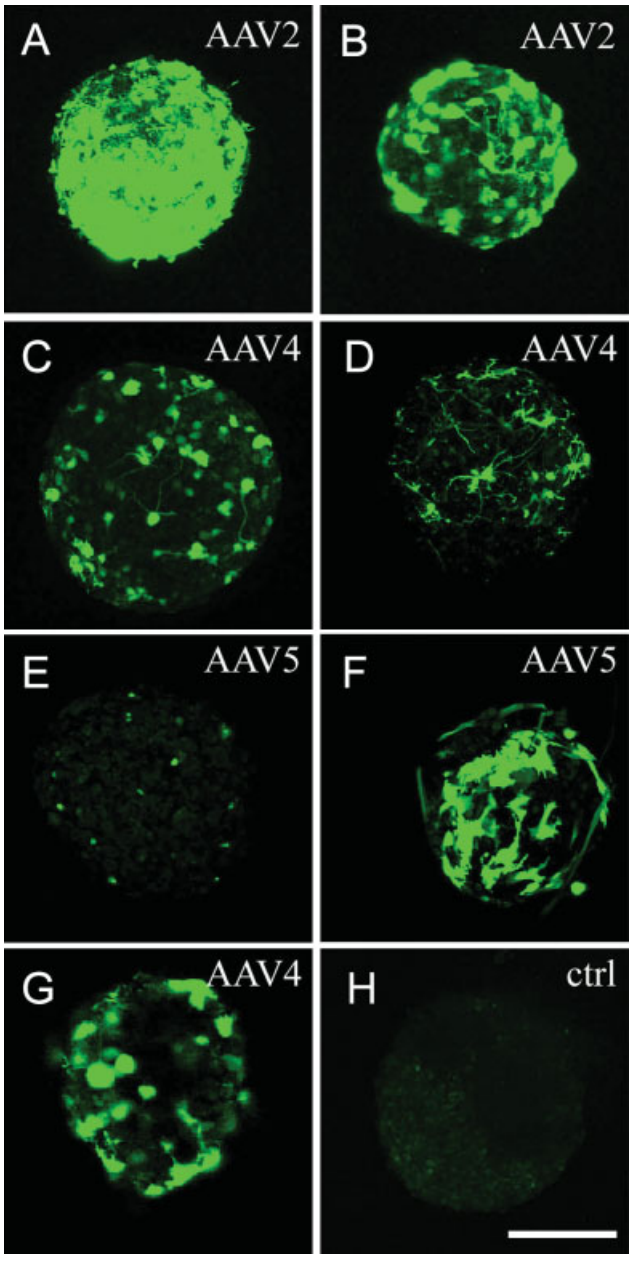

Figure 4. AAV serotypes 2, 4 and 5 transduce human glioblastoma spheroids *in vitro*. Human biopsy spheroids are effectively transduced by AAV. The figure shows AAV-infected spheroids obtained from three different patients. Confocal laser scanning microscopy (CLSM) was performed 2 weeks post-infection. (A) Spheroids obtained from patient 1, and infected with 2×10^8 AAV2-GFP genomes. CLSM was performed 6 weeks post-infection. (B) Spheroids obtained from patient 2, and infected with 2×10^8 AAV2-GFP genomes. CLSM was performed 2 weeks post-infection. (C) Spheroids obtained from patient 2, and infected with 2×10^8 AAV4-GFP genomes. CLSM was performed 2 weeks post-infection. (D) Spheroids obtained from patient 3, and infected with 2×10^9 AAV4-GFP genomes. CLSM was performed 6 weeks post-infection. (E) Spheroids obtained from patient 2, and infected with 2×10^8 AAV5-GFP genomes. CLSM was performed 2 weeks post-infection. (F) Spheroids obtained from patient 3, and infected with 1×10^{10} AAV5-GFP genomes. CLSM was performed 2 weeks post-infection. (G) One optical section from the central part of a glioblastoma spheroid from patient 1, 4 weeks post-infection with AAV4-GFP genomes. (H) Negative control from patient 2, CLSM performed after 2 weeks. Magnification: 125×; scale bar: 200 μm

DOI: 10.1002/jgm

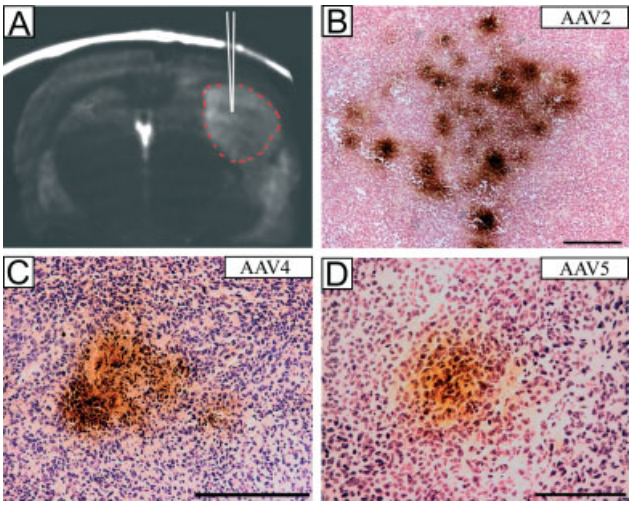

Figure 5. AAV serotypes 2, 4 and 5 transduce human glioblastoma xenograft tissue. (A) Magnetic resonance image (T1 weighted, with contrast enhancement) of a rat brain with a glioblastoma xenograft visible in the right cerebral hemisphere (outlined by red broken lines). AAV vector injections were performed into the same locality as used for spheroid implantation (indicated by white needle-tip). (B) Tumor sections immunostained against the AAV2 GFP transgene revealed clustered localization of transduced tumor cells in central areas of the xenografts. 2×10^9 vector genomes were injected. Magnification: 40×; scale bar: 250 μm. (C) Immunostaining against AAV4-GFP also showed clustered localization of transduced tumor cells in central tumor areas. 3×10^8 vector genomes were injected. Magnification: 100×; scale bar: 250 μm. (D) Similar results were also shown for immunostaining against AAV5-GFP. 2×10^8 vector genomes were injected. Magnification: 200×; scale bar: 100 μm

that neutralizing antibodies to a given AAV serotype may be present in humans [24]. Therefore, alternative AAV serotypes should be evaluated for use in patients where such antibodies are present. In addition, since each serotype may transduce the same tumor cell, these results reveal the potential for multiple or combinatorial application modalities using several different AAV vectors for repeated administrations.

In the panel of cell lines tested *in vitro*, we did detect differences in the numbers of cells that were transduced by each serotype. It is unlikely that competition by empty capsids accounts for these observations, as empty capsids were separated from DNA-containing capsids by CsCl centrifugation. Furthermore, these serotype vectors contain the same RSV promoter sequences and poly-A tail signalling elements. It is therefore not likely that the differences in transduction efficiency can be explained by the interference of individual cis-acting elements. One feasible interpretation is that differences in transduction efficiency may be related to differential binding, uptake and processing mechanisms specific to each serotype.

We prepared multicellular tumor spheroids from patient biopsies in order to study transduction efficiency and penetration in solid tumor tissue. Such three-dimensional, *in vitro* solid tumor preparations are closely related to the *in vivo* situation [42], and have recently been adapted by several investigators [47–49]. Previously, we have shown that AAV2, in contrast to adenovirus, penetrated and transduced deeply within spheroids [16]. Here we observed transgene-positive cells at the spheroid surface as well as in the more central layers of the spheroids, following infection with each of the three AAV serotypes. It is not likely that these central AAV-transduced cells were derived from positive cells at the outer periphery of the spheroids, since primary GBM spheroids do not exhibit extensive proliferation in short-term culture [50]. Thus, AAV4 and AAV5 vectors may be added to the short list of vectors that are able to penetrate and transduce beyond the surface layers of solid tumor tissue, in contrast to non-replicating adenoviral and retroviral vector systems [16,45,51–53].

To examine AAV serotype transduction *in vivo*, we modelled glioblastoma *in situ* by xenografting tumor spheroids derived from patient biopsies into nude rat brains. This model reflects the diverse phenotypes observed in glioblastoma multiforme *in situ*, and is distinct from xenografts derived from immortalized cell lines [44,54]. AAV-transduction was detected in small clusters within central parts of the tumor. As seen in Figure 5, there were also areas in the tumors where we could not identify transgene expression. The low transduction efficiency observed may be related to the loss of vector sequences from initially infected cells in the absence of integration, to the loss of transduced cells due to tumor necrosis, or to silencing of the RSV promoter *in vivo* [18,35]. In the mammalian brain, silencing of non-CNS promoters, such as cytomegalovirus (CMV), has been observed in the context of AAV-mediated gene transfer [55–57]. Hypermethylation has been suggested as a possible mechanism responsible for the observed effects [35]. Similar mechanisms may have resulted in silencing of the exogenous RSV promoters employed in these vectors. Attempts to localize the needle track in order to establish if the transgene-positive clusters coincided with the site of injection were unsuccessful since the area was re-populated by tumor cells.

Results obtained after AAV5 infection of tumor spheroids in culture (Figure 4) indicate that higher particle numbers of vector delivered results in the transduction of larger tissue areas. In the current setting, vector genomes in the range of 10^8–10^9 were injected. In recent studies, 10^{11}–10^{12} vector genomes were delivered to the CNS, which resulted in more widespread tissue transduction [36,58].

In experimental glioma models AAV vectors carrying the thymidine kinase suicide gene have initially shown significant therapeutic efficacy, and even regression of established tumors has been seen [59,60]. However, a more recent study has failed to reproduce these results [61]. Notably, all of these studies were performed using cell-line-based tumor xenografts. Therefore, to draw conclusions that are relevant to the clinical setting, we have evaluated the efficacy of AAV vectors used on patient biopsy material.

DOI: 10.1002/jgm

In conclusion, the present study shows that AAV serotypes 2, 4 and 5 are able to transduce human glioma cells *in vitro* as well as *in vivo*. This 'proof of principle' study reveals common properties for AAV 2, AAV4 and AAV5: (1) similar host ranges, (2) effective penetration in solid human tumor tissue, and (3) the capacity to transduce human biopsy-derived tumor xenografts *in vivo*. These data support the contention that AAV vectors may be developed as suitable gene delivery vehicles for cancer treatment. Even though the flow cytometric results showed a limited transduction efficacy in the cell lines, compared to AAV2, the spheroid data of AAV4 and AAV5 points to these serotypes as feasible alternatives to the AAV2 serotype. It should be noted that the titer used in the present study was relatively low. However, previous studies have shown that by increasing the viral titer, the transduction efficacy will increase [17]. Taking the cellular heterogeneity present in cancers into account, applying different AAV serotypes in concert or sequence could be a feasible way of enhancing transduction efficiency.

Acknowledgements

This work was supported by grants from the Norwegian Cancer Society, the University of Bergen, Captain Hermansen Fund, the Norwegian Health Ministry and Helse Vest, Haukeland University Hospital. The work has also been partly supported by the EU Integrated Project Angiotargeting (Contract no. 504743), and by the Intramural Research Program of the NIH, NHLBI. We thank Morten Lund-Johansen for assistance with surgical specimens, and Per Øyvind Enger for constructive comments to this manuscript. We are grateful to Ingvild Aukrust, Tomasz Furmanek and Tove Johansen for technical assistance.

References

1. Hemminki A. From molecular changes to customised therapy. *Eur J Cancer* 2002; **38**: 333–338.
2. Curiel DT. The development of conditionally replicative adenoviruses for cancer therapy. *Clin Cancer Res* 2000; **6**: 3395–3399.
3. Rainov NG, Kramm CM. Vector delivery methods and targeting strategies for gene therapy of brain tumors. *Curr Gene Ther* 2001; **1**: 367–383.
4. Smith-Arica JR, Bartlett JS. Gene therapy: recombinant adeno-associated virus vectors. *Curr Cardiol Rep* 2001; **3**: 43–49.
5. Smith RH, Kotin RM. Adeno-associated virus. In *Mobile DNA II*, Craig NL, Craigie R, Gellert M, *et al*. (eds). ASM Press: Washington DC, 2002; 905–923.
6. Gonzalves MAFV. Adeno-associated virus: from defective virus to effective vector. *Virol J* 2005; **2**: 43 (published online May 6). DOI: 10.1186/1743-422X-2-43.
7. Monahan PE, Samulski RJ. AAV vectors: is clinical success on the horizon? *Gene Ther* 2000; **7**: 24–30.
8. Janson C, McPhee S, Bilaniuk L, *et al*. Clinical protocol. Gene therapy of Canavan disease: AAV-2 vector for neurosurgical delivery of aspartoacylase gene (ASPA) to the human brain. *Hum Gene Ther* 2002; **13**: 1391–1412.
9. Flotte TR, Virella-Lowell I, Chesnut KA. Adeno-associated viral vectors for CF gene therapy. *Methods Mol Med* 2002; **70**: 599–608.
10. Kay MA, Manno CS, Ragni MV, *et al*. Evidence for gene transfer and expression of factor IX in haemophilia B patients treated with an AAV vector. *Nat Genet* 2000; **24**: 257–261.
11. Manno CS, Chew AJ, Hutchison S, *et al*. AAV-mediated factor IX gene transfer to skeletal muscle in patients with severe hemophilia B. *Blood* 2003; **101**: 2963–2972.
12. Ponnazhagan S, Curiel DT, Shaw DR, *et al*. Adeno-associated virus for cancer gene therapy. *Cancer Res* 2001; **61**: 6313–6321.
13. Veldwijk MR, Fruehauf S, Schiedlmeier B, *et al*. Differential expression of a recombinant adeno-associated virus 2 vector in human CD34+ cells and breast cancer cells. *Cancer Gene Ther* 2000; **7**: 597–604.
14. Kunke D, Grimm D, Denger S, *et al*. Preclinical study on gene therapy of cervical carcinoma using adeno-associated virus vectors. *Cancer Gene Ther* 2000; **7**: 766–777.
15. Hacker UT, Wingenfeld L, Kofler DM, *et al*. Adeno-associated virus serotypes 1 to 5 mediated tumor cell directed gene transfer and improvement of transduction efficiency. *J Gene Med* 2005; **7**: 1429–1438.
16. Enger PØ, Thorsen F, Lønning PE, *et al*. Adeno-associated vectors penetrate solid tumor tissue more effectively than adenoviral vectors. *Hum Gene Ther* 2002; **13**: 1115–1125.
17. Huszthy PC, Svendsen A, Wilson JM, *et al*. Widespread dispersion of adeno-associated virus serotype 1 and adeno-associated virus serotype 6 in the rat nervous system and in human glioblastoma multiforme xenografts. *Hum Gene Ther* 2005; **16**: 381–392.
18. Nakai H, Yant SR, Storm TA, *et al*. Extrachromosomal recombinant adeno-associated virus vector genomes are primarily responsible for stable liver transduction in vivo. *J Virol* 2001; **75**: 6969–6976.
19. McCarthy DM, Young SM Jr, Samulski RJ. Integration of adeno-associated virus (AAV) and recombinant AAV vectors. *Annu Rev Genet* 2004; **38**: 819–845.
20. Chiorini JA, Kim F, Yang L, *et al*. Cloning and characterization of adeno-associated virus type 5. *J Virol* 1999; **73**: 1309–1319.
21. Chiorini JA, Yang L, Liu Y, *et al*. Cloning of adeno-associated virus type 4 (AAV4) and generation of recombinant AAV4 particles. *J Virol* 1997; **71**: 6823–6833.
22. Gao GP, Alvira MR, Wang L, *et al*. Novel adeno-associated viruses from rhesus monkeys as vectors for human gene therapy. *Proc Natl Acad Sci U S A* 2002; **99**: 11854–11859.
23. Rutledge EA, Halbert CL, Russell DW. Infectious clones and vectors derived from adeno-associated virus (AAV) serotypes other than AAV type 2. *J Virol* 1998; **72**: 309–319.
24. Xiao W, Chirmule N, Berta SC, *et al*. Gene therapy vectors based on adeno-associated virus type 1. *J Virol* 1999; **73**: 3994–4003.
25. Grimm D, Kay MA. From virus evolution to vector revolution: use of naturally occurring serotypes of adeno-associated virus (AAV) as novel vectors for human gene therapy. *Curr Gene Ther* 2003; **3**: 281–304.
26. Qing K, Mah C, Hansen J, *et al*. Human fibroblast growth factor receptor 1 is a co-receptor for infection by adeno-associated virus 2. *Nat Med* 1999; **5**: 71–77.
27. Qing K, Hansen J, Weigel-Kelley KA, *et al*. Adeno-associated virus type 2-mediated gene transfer: role of cellular FKBP52 protein in transgene expression. *J Virol* 2001; **75**: 8968–8976.
28. Summerford C, Samulski RJ. Membrane-associated heparan sulfate proteoglycan is a receptor for adeno-associated virus type 2 virions. *J Virol* 1998; **72**: 1438–1445.
29. Summerford C, Bartlett JS, Samulski RJ. AlphaVbeta5 integrin: a co-receptor for adeno-associated virus type 2 infection. *Nat Med* 1999; **5**: 78–82.
30. Walters RW, Yi SM, Keshavjee S, *et al*. Binding of adeno-associated virus type 5 to 2,3-linked sialic acid is required for gene transfer. *J Biol Chem* 2001; **276**: 20610–20616.
31. Kaludov N, Brown KE, Walters RW, *et al*. Adeno-associated virus serotype 4 (AAV4) and AAV5 both require sialic acid binding for hemagglutination and efficient transduction but differ in sialic acid linkage specificity. *J Virol* 2001; **75**: 6884–6893.
32. DiPasquale G, Davidson BL, Stein CS, *et al*. Identification of PDGFR as a receptor for AAV-5 transduction. *Nat Med* 2003; **9**: 1306–1312.
33. Werbowetski T, Bjerkvig R, Del Maestro RF. Evidence for a secreted chemorepellent that directs glioma cell invasion. *J Neurobiol* 2004; **60**: 71–88.
34. Davidson BL, Stein CS, Heth JA, *et al*. Recombinant adeno-associated virus type 2, 4, and 5 vectors: transduction of variant cell types and regions in the mammalian central nervous system. *Proc Natl Acad Sci U S A* 2000; **97**: 3428–3432.

35. Tenenbaum L, Chtarto A, Lehtonen E, *et al*. Recombinant AAV-mediated gene delivery to the central nervous system. *J Gene Med* 2004; **6**: 212–222.
36. Burger C, Gorbatyuk OS, Velardo MJ, *et al*. Recombinant AAV viral vectors pseudotyped with viral capsids from serotypes 1, 2, and 5 display differential efficiency and cell tropism after delivery to different regions of the central nervous system. *Mol Ther* 2004; **10**: 302–317.
37. Tysnes BB, Thorsen F, Afione S, *et al*. Expression of heparan sulfate proteoglycan, integrin alpha V beta 5, and fibroblast growth factor receptor on malignant cell lines and human glioblastoma biopsy specimens. *Mol Ther* 2002; **5**(suppl 1): 47.
38. Chiorini JA, Wendtner CM, Urcelay E, *et al*. High-efficiency transfer of the T cell co-stimulatory molecule B7-2 to lymphoid cells using high-titer recombinant adeno-associated virus vectors. *Hum Gene Ther* 1995; **6**: 1531–1541.
39. Grimm D, Kern A, Rittner K, *et al*. Novel tools for production and purification of recombinant adeno-associated virus vectors. *Hum Gene Ther* 1998; **9**: 2745–2760.
40. Smith RH, Afione SA, Kotin RM. Transposase-mediated construction of an integrated adeno-associated virus type 5 helper plasmid. *Biotechniques* 2002; **33**: 204–206, 208, 210–211.
41. Alisky JM, Hughes SM, Sauter SL, *et al*. Transduction of murine cerebellar neurons with recombinant FIV and AAV5 vectors. *Neuroreport* 2000; **11**: 2669–2673, 2000.
42. Bjerkvig R, Tønnesen A, Laerum OD, *et al*. Multicellular tumor spheroids from human brain tumors maintained in organ culture. *J Neurosurg* 1990; **72**: 463–475.
43. Thorsen F, Ersland L, Nordli H, *et al*. Imaging of experimental rat gliomas using a clinical MR scanner. *J Neurooncol* 2003; **63**: 225–231.
44. Engebraaten O, Hjortland GO, Hirschberg H, *et al*. Growth of precultured human glioma specimens in nude rat brain. *J Neurosurg* 1999; **90**: 125–132.
45. Oyvind PE, Visted T, Thorsen F, *et al*. Retroviral transfection of the lacZ gene from Liz-9 packaging cells to glioma spheroids. *Int J Dev Neurosci* 1999; **17**: 665–672.
46. Sonmez H, Kokoglu E, Suer S, *et al*. Fibronectin and sialic acid levels in human meningiomas and gliomas. *Cancer Lett* 1995; **90**: 119–122.
47. Grill J, Lamfers ML, van Beusechem VW, *et al*. The organotypic multicellular spheroid is a relevant three-dimensional model to study adenovirus replication and penetration in human tumors in vitro. *Mol Ther* 2002; **6**: 609–614.
48. Lamfers ML, Grill J, Dirven CM, *et al*. Potential of the conditionally replicative adenovirus Ad5-Delta24RGD in the treatment of malignant gliomas and its enhanced effect with radiotherapy. *Cancer Res* 2002; **62**: 5736–5742.
49. Bauerschmitz GJ, Lam JT, Kanerva A, *et al*. Treatment of ovarian cancer with a tropism modified oncolytic adenovirus. *Cancer Res* 2002; **62**: 1266–1270.
50. Bjerkvig R, Høstmark J, Pedersen PH, *et al*. Tumor spheroids from biopsy specimens. In *Spheroid Culture in Cancer Research*, Bjerkvig R (ed). CRC Press: Boca Raton, 1992; 41–56.
51. Puumalainen AM, Vapalahti M, Agrawal RS, *et al*. Beta-galactosidase gene transfer to human malignant glioma in vivo using replication-deficient retroviruses and adenoviruses. *Hum Gene Ther* 1998; **9**: 1769–1774.
52. Sandmair AM, Loimas S, Poptani H, *et al*. Low efficacy of gene therapy for rat BT4C malignant glioma using intra-tumoral transduction with thymidine kinase retrovirus packaging cell injections and ganciclovir treatment. *Acta Neurochir Suppl* 1999; **141**: 867–873.
53. Benedetti S, Dimeco F, Pollo B, *et al*. Limited efficacy of the HSV-TK/GCV system for gene therapy of malignant gliomas and perspectives for the combined transduction of the interleukin-4 gene. *Hum Gene Ther* 1997; **8**: 1345–1353.
54. Engebraaten O, Bjerkvig R, Lund-Johansen M, *et al*. Interaction between human brain tumour biopsies and fetal rat brain tissue in vitro. *Acta Neuropathol* 1990; **81**: 130–140.
55. McCown TJ, Xiao X, Li J, *et al*. Differential and persistent expression patterns of CNS gene transfer by an adeno-associated virus (AAV) vector. *Brain Res* 1996; **713**: 99–107.
56. Lo WD, Qu G, Sferra TJ, *et al*. Adeno-associated virus-mediated gene transfer to the brain: duration and modulation of expression. *Hum Gene Ther* 1999; **10**: 201–213.
57. Klein RL, Meyer EM, Peel AL, *et al*. Neuron-specific transduction in the rat septohippocampal or nigrostriatal pathway by recombinant adeno-associated virus vectors. *Exp Neurol* 1998; **150**: 183–194.
58. Vite CH, Passini MA, Haskins ME, *et al*. Adeno-associated virus vector-mediated transduction in the brain. *Gene Ther* 2003; **10**: 1874–1881.
59. Okada H, Miyamura K, Itoh T, *et al*. Gene therapy against an experimental glioma using adeno-associated virus vectors. *Gene Ther* 1996; **3**: 957–964.
60. Mizuno M, Yoshida J, Colosi P, *et al*. Adeno-associated virus vector containing the herpes simplex virus thymidine kinase gene causes complete regression of intracerebrally implanted human gliomas in mice, in conjunction with ganciclovir administration. *Jpn J Cancer Res* 1998; **89**: 76–80.
61. Hadaczek P, Mirek H, Berger MS, *et al*. Limited efficacy of gene transfer in herpes simplex virus-thymidine kinase/ganciclovir gene therapy for brain tumors. *J Neurosurg* 2005; **102**: 328–335.

DOI: 10.1002/jgm